Available online at www.sciencedirect.com
SCIENCE DIRECT
Journal of Sound and Vibration 295 (2006) 988–998
JOURNAL OF SOUND AND VIBRATION
www.elsevier.com/locate/jsvi

Balancing energy to estimate damping parameters in forced oscillators

Jin-Wei Liang[a,*], Brian F. Feeny[b]

[a]Department of Mechanical Engineering, MingChi University of Technology, 84 Gung-Juan Rd., Taishan, Taipei County, Taiwan 24306, Taiwan
[b]Department of Mechanical Engineering, Michigan State University, 2328C, Engineering Bldg., East Lansing, MI 48824, USA

Received 28 April 2005; received in revised form 18 November 2005; accepted 31 January 2006
Available online 11 April 2006

Abstract

This study makes use of an energy balance to identify damping parameters in mechanical vibration systems. By balancing the energy input as registered in the force–displacement relationship of the real system against the energy lost theoretically in a damping model with unknown parameters, the identification algorithms are developed. We apply the estimation equations to both numerical and experimental systems, modeled with Coulomb plus viscous damping, at resonance to show the effectiveness and reliability of the new identification method. The equivalent viscous and dry-friction damping estimates obtained from the experimental system are compared to those obtained from the forced-resonance method to show their consistencies.

1. Introduction

Friction parameter estimation is based on the analysis of measured input and output responses. Our interest is in identifying parameters of basic friction models by making use of vibration properties. To this end, free vibration decrements have been exploited for systems with linear stiffness elements and "small" damping. Here, "small" damping means two things: the free response has sufficiently many extreme excursions that can be measured with good resolution; and the frequency of damped oscillation is approximately equal to the undamped natural frequency ω_n. The classic logarithmic decrement scheme for viscous friction identification goes back to Helmholtz [1] and Rayleigh [2], while the constant decrement [3] can be used for estimation of Coulomb damping.

Jacobsen and Ayre [4] developed an approximate scheme for estimating both viscous and dry friction quantities from the free-vibration decrements by noting that the viscous friction dominates in the large-amplitude responses, and that Coulomb friction dominates in the small-amplitude oscillations. An exact formulation for the simultaneous estimation of Coulomb and viscous friction in oscillators has since been derived [5–7].

*Corresponding author. Tel.: +886 2 29089899x4516; fax: +886 2 29041914.
E-mail addresses: liangj@ccsun.mit.edu.tw (J.-W. Liang), feeny@egr.msu.edu (B.F. Feeny).

0022-460X/$ - see front matter © 2006 Elsevier Ltd. All rights reserved.
doi:10.1016/j.jsv.2006.01.060

Free vibration decrements are not applicable if the damping is strong enough to preempt sufficient oscillations. As such, it makes sense to develop schemes for identifying friction parameters in forced oscillators. For instance, Stanway et al. [8] proposed identifying Coulomb and viscous damping parameters with a nonlinear least-squares scheme, which involves the on-line solution of several additional differential equations. Yao et al. [9] identified the Coulomb and viscous friction parameters by applying a recursive nonlinear least-squares algorithm. Chen and Tomlinson [10] proposed estimating damping parameters in nonlinear oscillators by utilizing the acceleration, velocity and displacement output and formulating the output in terms of series of frequency response functions. Tomlinson and Hibbert [11] applied the power dissipation to estimate Coulomb and hysteretic damping coefficients. Tomlinson [12] also measured the distortions in the complex receptance plots to identify damping parameters. Iourtchenko and Dimentberg [13] used stochastic averaging to identify nonlinear damping in-process when the excitation was random. Iourtchenko et al. [14], based on Dimentberg [15], applied a harmonic balance analysis to generate identification equations.

A scheme for extracting Coulomb and viscous friction parameters from forced oscillations based on the analytical solutions of Den Hartog [16] and Hundal [17] for the nonsticking response to harmonic excitations was formulated in our previous work [18]. We proposed an approximate forced-identification algorithm denoted as the analytical forced-resonance method. The analytical forced-resonance method employs an assumption of small viscous damping of the real system leading to a linear relationship between amplitudes of harmonic input and output motion. Analytical, numerical and experimental studies have shown the analytical forced-resonance method to be effective.

The limitations of the analytical forced-resonance method are that it is not applicable for damping which is not "small," it relies on analytical solutions of single-degree-of-freedom linear systems, and it does not treat friction models other than Coulomb plus viscous (see, for example, Refs. [19–24]). The need for analytical solutions can limit the identification of more complicated systems. Nonetheless, since the analytical forced-resonance method is based on an analytical solution, it can also serve as a benchmark in the continuing development of damping identification schemes for more general systems, for which analytical solutions are not available.

In this paper, we propose an energy balance as an alternative to using analytical solutions for identifying friction parameters. We apply the energy-balance formulation to systems with co-existing Coulomb and viscous friction as an example. There are other more advanced friction models that can capture complicated friction dynamics, such as the work of Soom et al. [25], the state-variable models of Rice [26], Deterich [27], and Ruina [28], the bristle models of Hassig and Friedland [24] and Canudas de Wit et al. [29], the normal vibration models of Tolstoi [30], Oden and Martins [21] and Dankowicwz [31], and the contact compliance models [22–24,32–35].

In developing the energy-balance method, the energy input of a physical system is registered in the force–displacement relationship. This energy input is balanced against the energy loss of a theoretical model, consisting of viscous damping and dry friction components. From this balance of energy, the estimation equations are derived, and applied to numerical and experimental systems in order to examine the reliabilities of the new identification method.

2. The energy-dissipation identification

The energy-dissipation identification method involves the balance between the energy dissipated by the friction force against the energy input to the system. This balance results in the "equivalent viscous and Coulomb damping" parameters, reminiscent to the traditional "equivalent viscous damping" concept seen in undergraduate textbooks, such as [36]. In the traditional approach, an equivalent viscous model replaces another nonlinear damping model such that there is an energy balance. The measured response amplitude and the nonlinear damping model are used together with a harmonic response assumption to compute the equivalent viscous damping coefficient. In this work, we suggest balancing energy using measured inputs and outputs to identify the coefficients of an assumed nonlinear damping model.

Consider a damped-forced oscillator with the following equation of motion:

$$m\ddot{x} + kx + F(x, \dot{x}) = a(t), \tag{1}$$

where m is the mass, k the stiffness, x the displacement, dots represent derivatives with respect to time, and $a(t)$ is the excitation. Multiplying (1) by $\mathrm{d}x$ and integrating along the motion path C yields the following energy-balance equation

$$\int_C \{m\ddot{x} + kx + F(x, \dot{x})\}\,\mathrm{d}x = \int_C a(t)\,\mathrm{d}x.$$

To assist the implementation of integration, the integration variable can be changed to time. Thus,

$$\int_t^{t+T_1} \{m\ddot{x} + kx + F(x, \dot{x})\}\dot{x}\,\mathrm{d}t = \int_t^{t+T_1} a(t)\dot{x}\,\mathrm{d}t.$$

Here T_1 indicates a finite time interval. We define

$$W_d = \int_t^{t+T_1} F(x, \dot{x})\dot{x}\,\mathrm{d}t; \quad W_a = \int_t^{t+T_1} a(t)\dot{x}\,\mathrm{d}t,$$
$$W_e = \int_t^{t+T_1} \{m\ddot{x} + kx\}\dot{x}\,\mathrm{d}t$$

so that Eq. (1) can be expressed as

$$W_d = W_a - W_e \tag{2}$$

representing a balance between the dissipated, applied energy, and the sum of the kinetic and elastic energy, respectively. The terms in Eq. (2) can be quantified if $x(t)$ (and its derivatives) and $a(t)$ are measured. Then, by integrating and balancing both sides of Eq. (2) while expressing $F(x, \dot{x})$ using an assumed friction model with unknown parameters, an identification equation for the parameters can be acquired. In order to improve the estimation accuracy, the excitation level can be varied to obtain more identification equations than the number of unknown parameters, so that the least-squares criterion can be applied. Details will be given later. While computing W_e requires acceleration, m and k, for bounded input and response, we have $W_e/W_d \to 0$ and $W_e/W_a \to 0$ as $T \to \infty$. Thus for long measured time histories, W_e can be neglected.

On the other hand, when $a(t)$ and $x(t)$ are periodic, one can integrate Eq. (2) over a cycle of periodic motion. In that case, the contribution of the conservative components of the oscillator, "$m\ddot{x} + kx$", is zero, so that the following energy-balance equation can be obtained

$$W_d = \int_t^{t+T} F(x, \dot{x})\dot{x}\,\mathrm{d}t = \int_t^{t+T} a(t)\dot{x}\,\mathrm{d}t = W_a, \tag{3}$$

where T represents the period of the response. Integrating and balancing both sides of Eq. (3), using measured data and a friction model to express $F(x, \dot{x})$ with unknown parameters, leads to an identification equation for the parameters. The mass and stiffness parameters need not be known for the estimation of damping parameters.

This paper focuses on the case for which the input is periodic. We will outline the details in an example.

2.1. Base-excited oscillator with Coulomb and viscous damping

A schematic diagram showing a base-excited oscillator together with damping components is presented in Fig. 1, in which the Coulomb friction and viscous damping are chosen to represent the damping effects existing in an industrial linear-bearing system [37]. The model shown in Fig. 1 differs from that of Hundal [17], with the viscous and Coulomb element between the mass and ground instead of parallel with the spring (i.e. between the moving base and the mass). The equation of motion of the oscillator can be written as

$$m\ddot{x} + c\dot{x} + kx + F_k\mathrm{sgn}(\dot{x}) = kY\cos\omega t, \tag{4}$$

where $F_k\mathrm{sgn}(\dot{x})$ represents Coulomb friction for pure sliding with no difference between the static and kinetic components, c is the viscous damping coefficient, and $kY\cos\omega t = a(t)$ represents the harmonic base input.

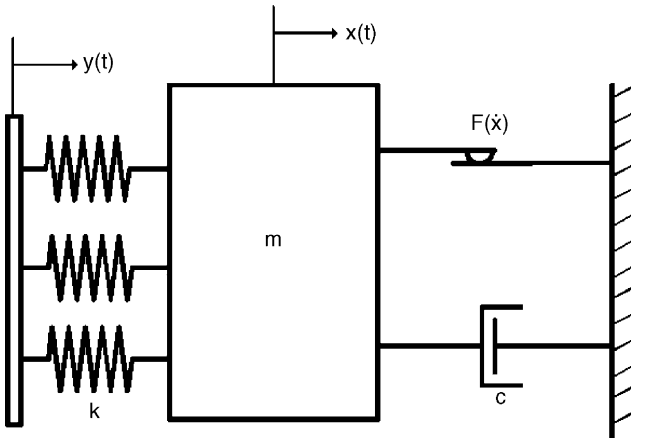

Fig. 1. A schematic diagram depicting a single-degree-of-freedom oscillator with viscous, Coulomb friction and base excitation.

Applying the right-hand side of Eq. (3) we acquire

$$W_a = \int_t^{t+T} a(t)\dot{x}\,\mathrm{d}t = \int_t^{t+T} ky\dot{x}\,\mathrm{d}t, \tag{5}$$

which is the energy supplied per cycle, determined by the measured motion signals $y(t)$ and $\dot{x}(t)$ and the stiffness k. In addition, the energy dissipated in the dual-damped oscillator during one forcing cycle is

$$W_d = \int_t^{t+T} F_k \operatorname{sgn}(\dot{x})\dot{x}\,\mathrm{d}t + \int_t^{t+T} c\dot{x}\dot{x}\,\mathrm{d}t = \alpha F_k + \beta c, \tag{6}$$

where α and β are defined by the time integrals

$$\alpha = \int_t^{t+T} \operatorname{sgn}(\dot{x})\dot{x}\,\mathrm{d}t, \quad \beta = \int_t^{t+T} \dot{x}^2\,\mathrm{d}t. \tag{7}$$

As such, Eq. (3), $W_d = W_a$, leads to

$$\alpha F_k + \beta c = \int_t^{t+T} ky\dot{x}\,\mathrm{d}t. \tag{8}$$

Thus, the model of the energy dissipated by the damping forces of the physical system can be balanced against the energy supplied to the oscillator to produce a linear equation in the assumed damping coefficients. Multiple test measurements, $x_i(t)$ and $y_i(t)$, $i = 1,\ldots,n$, will lead to multiple coefficients α_i, β_i, and W_{ai}, i.e. multiple versions of Eq. (8), which can be written in matrix form as

$$\underline{W} = A\,\underline{p}, \tag{9}$$

where $\underline{W}$ is a vector of elements W_{ai}, A is a matrix for which each row i has the pair of values α_i, β_i, and $\underline{p} = [F_k, c]^{\mathrm{T}}$ is the vector of unknown parameters. The least-squares solution is

$$\underline{p} = (A^{\mathrm{T}}A)^{-1}A^{\mathrm{T}}\,\underline{W} \tag{10}$$

provides an estimate of the parameters, along with a residual $\underline{r} = A\,\underline{p} - \underline{W}$ that is generally nonzero. The residual can serve as an indicator of the quality of the damping model. In this case, it tells whether "$c\dot{x} + F_k \operatorname{sgn}(\dot{x})$" can closely represent $F(x, \dot{x})$ occurring at the contact interfaces [38]. Since the coefficients are obtained by integration, high-frequency noise is expected to be filtered, but low frequency noise can have more influence.

Dividing Eq. (8) by α_i, we see that a plot of W_{ai}/α_i data versus β_i/α_i data is expected to be a straight line, with a slope of c and an intercept of F_k. (The slope and intercept of the affine least-squares fit of the data in this plot produces a numerically different, and slightly less effective, estimation of the parameters, but allows for a visualization of the linearity of the data.)

2.2. Harmonic input and response

In the special case, when the input is harmonic, and the response is nearly so, it may make sense to make a harmonic approximation to Eq. (8). Substituting $ky(t) = kY\cos\omega t$, $x(t) = X\cos(\omega t - \phi)$, and $\dot{x}(t) = -\omega X\sin(\omega t - \phi)$ into Eqs. (7) and (8), and dividing by X, yields

$$\pi kY\sin\phi = 4F_k + \pi c\omega X. \tag{11}$$

Defining $x_k = F_k/k$, $\omega_n^2 = k/m$, $2\zeta\omega_n = c/m$, and $r = \omega/\omega_n$, we can rewrite Eq. (11) as

$$\pi Y\sin\phi = 4x_k + 2\pi\zeta Xr. \tag{12}$$

Eq. (11) would be used if the base excitation (or the applied force), ky, were known, while more likely Eq. (12) would be used if ω_n and y were known. Eq. (12) indicates a linear relationship between the input and output amplitudes in which the slope and intercept lead to estimates of the viscous damping factor ζ and the dry-friction parameter x_k.

The estimation strategy is to generate coefficients of Eqs. (11) or (12) for many input–output cases, perform a least squares fit to a straight line, and obtain the damping parameters from the slope and intercept.

At resonance, $r = 1$, and if we assume both ϕ_1 and ϕ_2 are approximately equal to $\pi/2$, then

$$\pi Y = 4x_k + 2\pi\zeta X \tag{13}$$

represents a very simple identification equation.

If there are two sets of data, Eq. (13) can be solved to obtain expressions for x_k and ζ. It can be shown that this estimation for ζ is the same as that of the analytical forced-resonance method [18], developed from analytical response expressions at resonance. In this energy-balance formulation, we have made assumptions of harmonic response with a 90° phase angle for various input levels at the same excitation frequency. In the forced-resonance method case, we made a "small ζ" assumption, neglecting ζ^2 effects. The equation for x_k in the two-point harmonic energy-balance estimation at resonance and that obtained by the two-point analytical forced resonance method (this quantity was denoted as x_f in [18]) differ by a factor of $x_k/x_f = G\pi\zeta/2$, where

$$G \cong \frac{\sinh\zeta\pi}{\cosh\zeta\pi - 1}$$

for small ζ. Indeed, as $\zeta \to 0$, $G \to 2/\pi\zeta$. Hence, the x_k estimations and the forced-resonance analytical method converge as ζ decreases. This comment should be taken cautiously, since the Coulomb-only resonant response is unbounded [16]. However, it does suggest that the results for x_k should be similar between the analytical scheme and the harmonic energy-balance scheme if ζ is small.

The major difference between the energy balance and the analytical response methods is that the analytical response is needed in the latter case, but not for the former case. Thus, the energy balance method can be applied to more general systems, such as those with nonlinear stiffnesses, or, for example, quadratic damping laws. The form of Eqs. (8) or (12) depends on the damping model.

3. Numerical examples

We look at numerical examples using both the general integrated energy balance (IEB) and the harmonic energy balance (HEB) expressions. For comparison with the analytical method [18], we are interested to examine the applicability on and off resonance, and with slip and stick–slip.

3.1. Slipping motion

The parameters corresponding to Eq. (4) were $k = 100.0$; $m = 1.0$; $c = 4.0$ and $F_k = 2.0$. Hence $\zeta = 0.2$ $x_k = 0.02$. We excited the system at resonance, i.e., $\omega_1 = \omega_n = 10.0$, and the excitation levels Y were 0.2, 0.4, 0.8, and 1.0. For the harmonic balance, we used the analytical expression presented in Den Hartog's work [16] to obtain the response amplitudes $X = 0.43611762$, 0.93613738, 1.93614725, and 2.43614923. A numerical integration was also monitored to cross check if the pure-sliding motion indeed occurred.

For the HEB at resonance, the input–output amplitudes of four responses were processed to form Eq. (13). A straight line was fit to the X, Y data, and from the slope and intercept, we obtained the estimates $\tilde{\zeta}_{\mathrm{HEB}} = 0.19999708$ and $\tilde{x}_{k\mathrm{HEB}} = 0.020069475$. The mean of the absolute values of residuals in Eq. (13), normalized by the values of πY, was 5.10e-6. The source of the error includes the assumption that the motion is a single harmonic with an amplitude of Den Hartog's peak response solution and a phase of $\pi/2$, as well as the round-off in the peak response numerals.

To test the IEB method, we used a stiff, low-order ordinary differential equation solver of Bogacki and Shampine (ode23tb) provided in MATLAB (a commercial software) to numerically integrate Eq. (4) at a constant sampling rate after converting to first-order form [39]. Simpson's rule was used to obtain W_{ai}, α_i and β_i from an arbitrary cycle of the signals.

The least-squares estimation by Eq. (10) is $\tilde{\zeta}_{\mathrm{IEB}} = 0.200002$ and $\tilde{x}_{k\mathrm{IEB}} = 0.0199942$. The mean of the absolute values of the residuals (errors in each of Eq. (9)) normalized by the right-hand side of Eq. (9), was 8.9e-6, for numerically integrated noise-free numerical data with a perfect model. The plot of W_{ai}/α_i data versus β_i/α_i data was indistinguishable from a straight line.

Although the time-domain output signals are not shown here, they were dominantly sinusoidal. To verify this, we used the fast Fourier transform to check the power spectrum of the output amplitude response. The fundamental frequency differed from the harmonics by more than 120 dB.

We also tried the off-resonance case. The accuracy of the IEB method in the off-resonance regime could be nearly as good as the resonant case, while the accuracy of the HEB method slightly deteriorated in the off-resonance case. For instance, given the same parameters as those listed at the beginning of this section except that $\omega_1 = 12.0$ instead of 10.0, the HEB gave $\tilde{\zeta}_{\mathrm{HEB}} = 0.20851216$ and $\tilde{x}_{k\mathrm{HEB}} = 0.01199999$. The mean of the absolute values of residuals in Eq. (12), normalized by the values of $\pi Y \sin\phi$, was 3.24e-4. In contrast with the HEB method, the least-squares solution from the IEB approach is $\tilde{\zeta}_{\mathrm{IEB}} = 0.20001583$ and $\tilde{x}_{k\mathrm{IEB}} = 0.02008800$, with a mean of normalized residual absolute values of 2.76e-4. The method based on Den Hartog's analytical solution is more complicated to formulate off resonance, giving the energy balance added appeal over the analytical identification method [18].

3.2. Stick–slip motion

To induce sticking, we increased the dry friction force and then integrated Eq. (4) directly with $m = 1.0$, $F_k = 8.0$, $c = 4.0$, $k = 100.0$, and $\omega = 10.0$. Hence $\omega_n = 10.0$, $\zeta = 0.2$, and $x_k = 0.08$. The excitation levels Y were 0.09, 0.10, 0.11, and 0.12, and the response "amplitudes" were 0.002669, 0.011102, 0.025675, and 0.045560.

In implementing the harmonic balance identification Eq. (13), the phase between the excitation and response is needed, for which there is no clear definition since higher harmonics are significant during stick–slip motion. Therefore, we excited the system at resonance and assumed the phase angle to be $\pi/2$ radians, as the pure viscous case at resonance. A line was fit to the X, Y data, whence the slope and intercept produced the estimates $\tilde{\zeta}_{\mathrm{HEB}} = 0.3383$ and $\tilde{x}_{k\mathrm{HEB}} = 0.0712$. The mean of the absolute values of the residuals in Eq. (13) normalized by πY was 1.90e-2.

The phase issue prompts us to turn to the more general IEB. Because the integration expressions in Eqs. (3), (5), (6) all involve products of the velocity signal, the integrands become zero when sticking condition occurs. The least-squares estimation of the IEB method corresponding to the stick–slip data gives $\tilde{\zeta}_{\mathrm{IEB}} = 0.200233$ and $\tilde{x}_{k\mathrm{IEB}} = 0.079984$. The mean of the absolute values of the normalized residuals was 2.35e-4.

The integrated method is more appropriate in this case since stick–slip responses deviate significantly from the pure-harmonic approximation. An FFT test indicates that the most distorted case corresponding to four different excitation levels has the fundamental frequency 20 dB larger than other higher harmonics compared to the slip case in which a 120 dB difference appears.

4. Experiments

Our experimental system consists of two linear-bearing systems (THK SR20UU) with four linear motion (LM) blocks, an electromagnetic shaker with a power amplifier (Brüel & Kjær 4809 and 2706), two LVDTs

with signal conditioners (Rabinson-Halpern Co., Model 210A-0500), an accelerometer with a charge-type amplifier (Brüel & Kjær 4371 and 2635), and a data-acquisition system (NI-AT-MIO-16E-10 and LabVIEW). A photograph of the experimental set-up illustrating the linear-bearing system, the electromagnetic shaker, the base-excited plate, the helical springs, the LVDTs, and the accelerometer, is presented in Fig. 2.

In Fig. 2, the LVDTs were used to sense the displacement signals of the sliding mass and the base excitation, whereas an accelerometer was adopted to check if the response was close to the pure-sliding motion. Mechanical parameters of this experimental rig were $m = 1.042\,\text{kg}$, $k = 1568\,\text{N/m}$, $\omega_n = 6.2\,\text{Hz}$. The resolution of LVDTs after quantization in the data-acquisition process was about 3 μm. The data-acquisition system consisted of a PC and the LabVIEW software.

Experimentally, the process required to implement the identification scheme included (a) finding the system's resonance (b) obtaining steady-state responses for various input levels, Y_i (c) measuring input and output displacements x_i and y_i, (d) integrating energy coefficients, or extracting displacement amplitudes X_i and Y_i, and (e) seeking the least-squares solution of Eqs. (9) or (13).

Estimates obtained from the energy balance method will be compared to those obtained using the forced-resonance method [18] and the free-vibration decrement method. Finally, in Ref. [18], the friction force was measured, and the resulting dry-friction force level (comparable to the $\text{sgn}(\dot{x})$ coefficient F_k) was about 3.6 N, with evidence of some dynamical friction also involved [18,22].

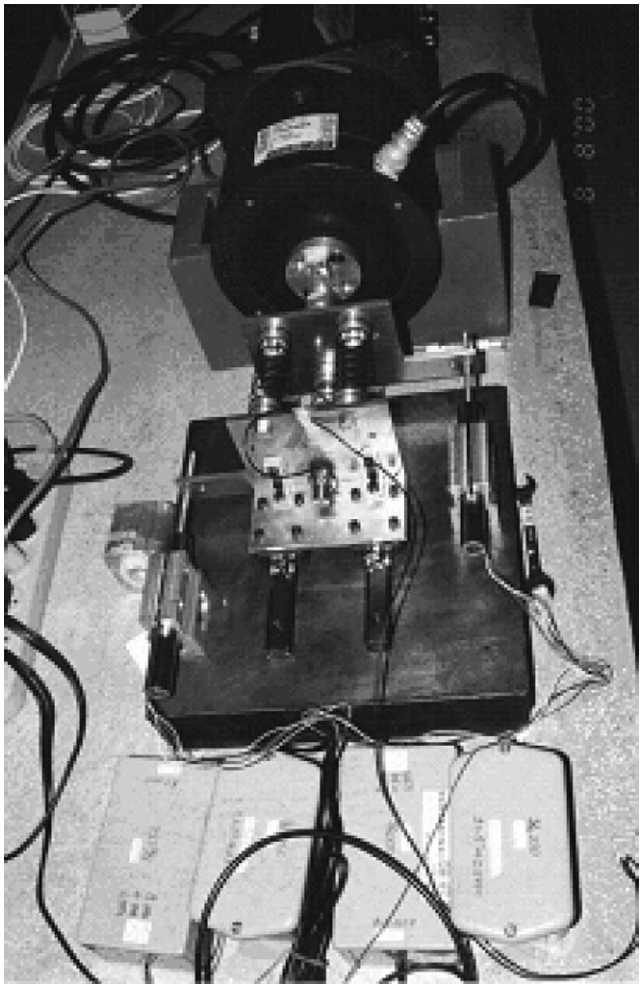

Fig. 2. A photograph of the experimental set-up illustrating the linear-bearing systems, the electromagnetic shaker, the LVDTs, etc.

4.1. Slip response at resonance

First we apply the harmonic approximation. The experimental (Y_i, X_i) input and response amplitude data shown in Fig. 3 were obtained from the experimental linear-bearing system excited approximately at the resonant frequency [18]. There are totally 100 pairs of input and output amplitudes shown in Fig. 3. Every small square shown in this figure indicates one pair of input and output amplitudes, and every input or output amplitude was averaged over more than 10 forcing periods at steady state [18]. Lines connect the points chronologically as recorded, and thus it seems that the intercept varies slowly, but not the slope (which varies a bit with amplitude), suggesting a slow variation in the dry-friction coefficient.

Recall (Section 2) that the estimates of the viscous parameters corresponding to data shown in Fig. 3 are exactly the same for both the HEB and analytical methods at resonance. The estimates of the viscous damping parameters are listed in Table 1. These estimates are obtained by first applying the least-squares fit of Eq. (13) to the whole data set, the lower 4/5, 3/5 and 2/5 of the data set. (The reason for doing this is that that *X, Y* plot seems to depart from a straight line for large amplitudes, suggesting a large-amplitude departure of the model, either in the harmonic assumption e.g. due to nonlinear stiffness, or in unmodeled damping effects [18].) The dry-friction estimates were then calculated according to Eq. (13) using the identified viscous-damping parameter together with the individual intercept of the linear squares fits. The results are also shown in Table 1.

Next we apply the IEB. The α_i, β_i, and W_{ai} were determined by integrating the experimental signals. The experimental response amplitude actually fluctuated on a small scale. Hence, the integrations were performed over about twelve forcing periods. The input levels were $Y = 4.318$, 4.910, 5.376, 5.665, and 6.090 mm, in the range of the lower third of the data for the slip case. The least squares estimation corresponding to the slip

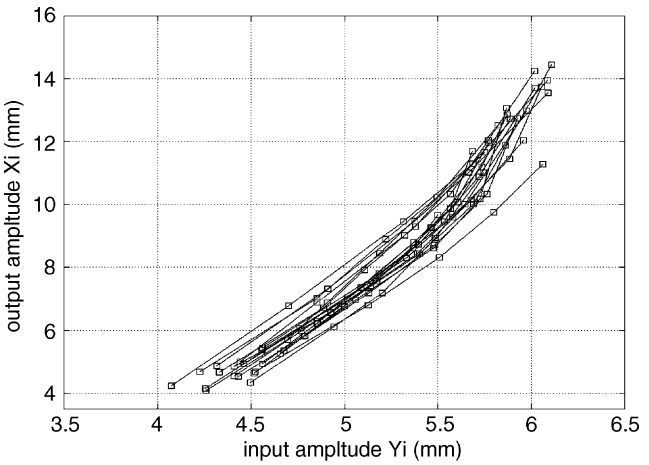

Fig. 3. The experimental input–output amplitudes measured nearly at the system's resonance.

Table 1
Experimental estimates of damping parameters of the linear-bearing system

Data	Both methods $\tilde{\zeta}$	Analytical method $\tilde{F}_{\mathrm{AM}}$	Energy method $\tilde{F}_{\mathrm{HEB}}$
Whole data set	$\tilde{\zeta}_1 = 0.0987$	$\tilde{F}_{\mathrm{AM1}} = 4.38$	$\tilde{F}_{\mathrm{HEB1}} = 4.38$
The 4/5 of the whole data set	$\tilde{\zeta}_{4/5} = 0.1143$	$\tilde{F}_{\mathrm{AM4/5}} = 4.12$	$\tilde{F}_{\mathrm{HEB4/5}} = 4.13$
The 3/5 of the whole data set	$\tilde{\zeta}_{3/5} = 0.1263$	$\tilde{F}_{\mathrm{AM3/5}} = 3.95$	$\tilde{F}_{\mathrm{HEB3/5}} = 3.96$
The 2/5 of the whole data set	$\tilde{\zeta}_{2/5} = 0.1424$	$\tilde{F}_{\mathrm{AM2/5}} = 3.73$	$\tilde{F}_{\mathrm{HEB2/5}} = 3.75$
The free-decrement method	$\tilde{\zeta}_{\mathrm{FDM}} = 0.1367$	$\tilde{F}_{\mathrm{FDM}} = 3.52$	

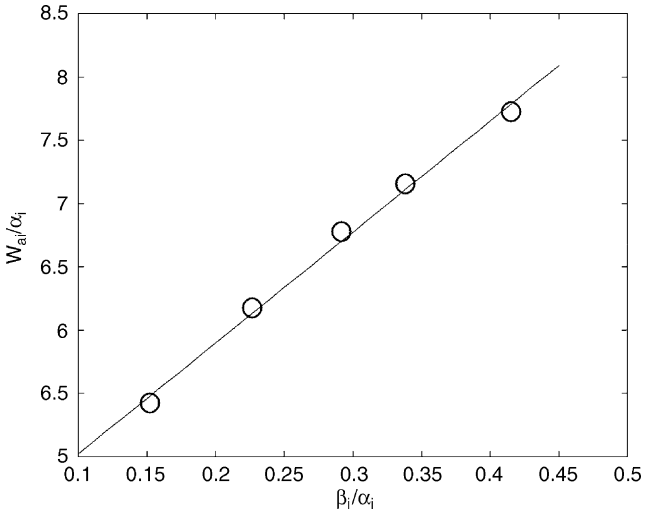

Fig. 4. Data distribution of slip response experiments for the IEB.

data gives $\tilde{\zeta}_{\mathrm{IEB}} = 0.103$ and $\tilde{F}_{k\mathrm{IEB}} = 4.29\,\mathrm{N}$. Both are very close to the slip estimations based on the entire slip data set, which are slightly low for ζ and slightly high for F_k compared to the free-vibration decrement method and the friction measured in Ref. [18]. The mean of the absolute values of normalized residuals was 0.00886. The data is visually close to the anticipated linear profile (Fig. 4).

4.2. Stick–slip response

We applied the IEB method to a mixed set of stick–slip and pure-sliding response signals. The test conducted consisted of four excitation levels, $Y = 2.570$, 2.625, 2.914, and 3.101 mm, at an excitation frequency of $\omega = 5.97\,\mathrm{Hz}$, slightly below resonance. Among these excitations, the stick–slip case corresponded to the lowest excitation level, whereas the pure-sliding cases corresponded to the other higher excitations. The least-squares estimation corresponding to this mixed set of data gives $\tilde{\zeta}_{\mathrm{IEB}} = 0.0873$ and $\tilde{F}_{k\mathrm{IEB}} = 3.23\,\mathrm{N}$, slightly low on both parameters as compared to the slip data and the free-vibration decrement estimation, but still at the right order for a rough approximation. The mean of the absolute values of normalized residuals of Eq. (9) was 0.0137.

5. Conclusion

This paper presents an algorithm for identifying damping information in forced vibration systems. The identification is based on a balance between dissipated energy and energy input. The input energy is obtained from measurements of the input and output displacement. This applied energy per cycle of response is balanced against the dissipated energy, formulated from the damping model. Balancing the measured energy input with the formulated loss leads to parameter identification equations.

The input and output signals are integrated to create numerical coefficients in the identification equations, which are then solved for the parameters in the least-squares sense. If the response is assumed to be harmonic, the input energy is a function of input and output amplitudes, frequency and phase, and the identification equations simplify, omitting the need for integrated coefficients. This, however, is at the cost of accuracy, which shows in some examples.

The harmonic response approximation works very well for the simulated and experimental linear oscillators with Coulomb plus viscous friction in sliding motion. For the simulated case this was successful on resonance. The more general integrated energy method not only worked on the on and off-resonance sliding cases, it also worked on the numerical and experimental examples with stick–slip responses.

The advantages of the energy balance approach for damping estimation are that it is founded on a simple concept, it is easy to apply, it does not require an analytical solution of the system, it does not require knowledge of the mass and stiffness (except in converting between ζ and c, and x_k and F_k), it does not require iterations, and it is theoretically applicable to a class of systems with linear and nonlinear stiffness for which the damping model consists of basis functions and is linear in the coefficients of basis functions. The latter statement was only supported, in this paper, in an example with linear stiffness and Coulomb plus viscous, for which the damping basis functions were $\mathrm{sgn}(\dot{x})$ and $\dot{x}$.

The harmonic energy-balance method described in this paper can be modified slightly to accommodate other friction and damping models. Work is underway on identifying a compliant-contact friction model.

Acknowledgments

Author J.-W. Liang was supported by the National Science Council (NSC892212E131005) of the Republic of China, Taiwan.

References

[1] H.L.F. Helmholtz, On the sensations of tone as physiological basis for the theory of music, in: A.J. Ellis (Ed.), *Die Lehre von den Tonempfindungen (first edition published in 1863)*, fourth ed., Dover, New York, 1877, p. 406.
[2] L. Rayleigh, 1877, *The Theory of Sound*, Vol. 1, Dover, New York, 1945, pp.46–51 (reprinted).
[3] H. Lorenz, Lehrbuch der Technischen Physik. *Technische Mechanik Starrer Gebilde, Erster Band*. Verlag von Julius Springer, Berlin, 1924.
[4] L.S. Jacobsen, R.S. Ayre, *Engineering Vibrations*, McGraw-Hill, New York, 1958.
[5] A. Watari, Kikai-rikigaku, Kyouritsu (publisher), 1969.
[6] B.F. Feeny, J.-W. Liang, A decrement method for the simultaneous estimation of Coulomb and viscous friction, *Journal of Sound and Vibration* 195 (1) (1996) 149–154.
[7] J.-W. Liang, B.F. Feeny, Identifying Coulomb and viscous friction from free-vibration decrements, *Nonlinear Dynamics* 16 (1998) 337–347.
[8] R. Stanway, J.L. Sproston, N.G. Stevens, A note on parameter estimation in nonlinear vibrating systems, *Proceedings of the Institution of Mechanical Engineers* 199 (C1) (1985) 79–84.
[9] G.Z. Yao, G. Meng, T. Fang, Parameter estimation and damping performance of electro-rheological dampers, *Journal of Sound and Vibration* 204 (4) (1997) 575–584.
[10] Q. Chen, G.R. Tomlinson, Parametric identification of systems with dry friction and nonlinear stiffness using a time series model, *Journal of Vibration and Acoustics* 118 (1996) 252–263.
[11] G.R. Tomlinson, J.H. Hibbert, Identification of the dynamic characteristics of a structure with Coulomb friction, *Journal of Sound and Vibration* 64 (2) (1979) 233–242.
[12] G.R. Tomlinson, An analysis of the distortion effects of Coulomb damping on the vector plots of lightly damped system, *Journal of Sound and Vibration* 71 (3) (1980) 443–451.
[13] D.V. Iourtchenko, M.F. Dimentberg, In-service identification of nonlinear damping from measured random vibration, *Journal of Sound and Vibration* 255 (3) (2002) 549–554.
[14] D.V. Iourtchenko, L. Duval, M.F. Dimentberg, The damping identification for certain SDOF systems, *Proceedings of the SECTAM-XX, Developments in Theoretical and Applied Mechanics*, April 16–18, Callaway Gardens, Pine Mountain, GA, 2002, pp. 535–538.
[15] M.F. Dimentberg, Determination of nonlinear damping function from forced vibration test of a SDOF system, *Mechanica Tverdogo Tela* (2) (1968) 32–34 (in Russian).
[16] J.P. Den Hartog, Forced vibration with combined Coulomb and viscous damping, *Transactions of the American Society of Mechanical Engineering* 53 (1931) 107–115.
[17] M.S. Hundal, Response of a base excited system with Coulomb and viscous friction, *Journal of Sound and Vibration* 64 (1979) 371–378.
[18] J.-W. Liang, B.F. Feeny, Identifying Coulomb and viscous friction in forced dual-damped oscillators, *Journal of Vibration and Acoustics* 126 (1) (2004) 118–125.
[19] R.A. Ibrahim, Friction-induced vibration chatter, squeal, and chaos: part I—mechanics of friction, friction-induced vibration, chatter, squeal, and chaos, *ASME Proceedings* DE-49 (1992) 107–121.
[20] B. Armstrong-Hélouvry, P. Dunpont, C. Canudas De Wit, A survey of models, analysis tools and compensation methods for the control of machines with friction, *Automatica* 30 (7) (1994) 1083–1138.
[21] J.T. Oden, J.A.C. Martins, Models and computational methods for dynamic friction phenomena, *Computer Mechanics in Applied Mechanics and Engineering* 52 (1-3) (1985) 527–634.
[22] J.-W. Liang, B.F. Feeny, Dynamical friction behavior in a forced oscillator with a compliant contact, *Journal of Applied Mechanics* 65 (1) (1998) 250–257.

[23] N. Hinrichs, M. Osetreich, K. Popp, On the modeling of friction oscillator, *Journal of Sound and Vibration* 216 (3) (1998) 435–459.
[24] D.A. Haessig, B. Friedland, On the modeling and simulation of friction, *Journal of Dynamic Systems, Measurement and Control* 113 (1991) 354–362.
[25] D.P. Hess, A. Soom, Friction at a lubricated line contact operating at oscillating sliding velocities, *Journal of Tribology* 112 (1990) 147–152.
[26] J.R. Rice, A.L. Ruina, Stability of steady friction slipping, *Journal of Applied Mechanics* 50 (1983) 343–349.
[27] J. H. Dieterich, Micro-mechanics of slip instabilities with rate- and state-dependent friction, *Volume Fall Meeting Abstract, 324*, Eos, Trans., Am. Geophys. Union, 1991.
[28] A. Ruina, Friction Laws and Instabilities: A Quasistatic Analysis of Some Dry Frictional Behavior, PhD Thesis, Division of Engineering, Brown University, 1980.
[29] C. Canudas de Wit, H. Olsson, K.J. Astrom, P. Lischinsky, A new model for control of systems with friction, *IEEE Transactions on Automatic Control* 40 (3) (1995) 419–425.
[30] D.M. Tolstoi, Significance of the normal degree of freedom and natural normal vibrations in contact friction, *Wear* 10 (1967) 199–213.
[31] H. Dankowicz, On the modeling of dynamic friction phenomena, *Zeitschrift fuer angewandte Mathematik und Mechanik* 79 (6) (1999) 399–409.
[32] A. Harnoy, B. Friedland, B.H. Rachor, Modeling and simulation of elastic and friction force in lubricated bearing for precise motion control, *Wear* 172 (1994) 155–165.
[33] A.J. McMillan, A non-linear friction model for self-excited vibration, *Journal of Sound and Vibration* 205 (3) (1997) 323–335.
[34] R.V. Kappagantu, B.F. Feeny, Part 1: dynamical characterization of a frictionally excited beam, *Nonlinear Dynamics* 22 (4) (2000) 317–333.
[35] R.V. Kappagantu, B.F. Feeny, Part 2: proper orthogonal modal modeling of a frictionally excited beam, *Nonlinear Dynamics* 23 (1) (2000) 1–11.
[36] W.T. Thomson, M.D. Dahleh, *Theory of Vibration with Applications*, Prentice-Hall, New Jersey.
[37] THK, *Linear Motion System*, THK Co., Ltd., Catalog No.200-1AE, Tokyo, Japan, 1996.
[38] J. Beck, J.K. Arnold, *Parameter Identification in Engineering and Science*, Wiley, New York, 1977.
[39] P. Bogacki, L.F. Shampine, A 3(2) pair of Runge–Kutta formulas, *Applied Mathematics Letters* 2 (1989) 1–9.